

Exploring the origin of the internal rotational barrier for molecules with one rotatable dihedral angle

Shubin Liu,^{1,2,a),b)} Niranjan Govind,³ and Lee G. Pedersen^{4,5,a),c)}

¹*Renaissance Computing Institute, University of North Carolina, Chapel Hill, North Carolina 27599-3455, USA*

²*Research Computing Center, University of North Carolina, 211 Manning Drive, Chapel Hill, North Carolina 27599-3420, USA*

³*William R. Wiley Environmental Molecular Sciences Laboratory, Pacific Northwest National Laboratory, Richland, Washington 99352, USA*

⁴*Laboratory of Structural Biology, National Institute of Environmental Health Sciences, Research Triangle Park, P.O. Box 12233, North Carolina 27709, USA*

⁵*Department of Chemistry, University of North Carolina, Chapel Hill, North Carolina 27599-3290, USA*

(Received 9 June 2008; accepted 7 August 2008; published online 3 September 2008)

Continuing our recent endeavor, we systematically investigate in this work the origin of internal rotational barriers for small molecules using the new energy partition scheme proposed recently by one of the authors [S. B. Liu, *J. Chem. Phys.* **126**, 244103 (2007)], where the total electronic energy is decomposed into three independent components, steric, electrostatic, and fermionic quantum. Specifically, we focus in this work on six carbon, nitrogen, and oxygen containing hydrides, CH_3CH_3 , CH_3NH_2 , CH_3OH , NH_2NH_2 , NH_2OH , and H_2O_2 , with only one rotatable dihedral angle $\angle\text{H}-\text{X}-\text{Y}-\text{H}$ ($\text{X}, \text{Y}=\text{C}, \text{N}, \text{O}$). The relative contributions of the different energy components to the total energy difference as a function of the internal dihedral rotation will be considered. Both optimized-geometry (adiabatic) and fixed-geometry (vertical) differences are examined, as are the results from the conventional energy partition and natural bond orbital analysis. A wealth of strong linear relationships among the total energy difference and energy component differences for different systems have been observed but no universal relationship applicable to all systems for both cases has been discovered, indicating that even for simple systems such as these, there exists no omnipresent, unique interpretation on the nature and origin of the internal rotation barrier. Different energy components can be employed for different systems in the rationalization of the barrier height. Confirming that the two differences, adiabatic and vertical, are disparate in nature, we find that for the vertical case there is a unique linear relationship applicable to all the six molecules between the total energy difference and the sum of the kinetic and electrostatic energy differences. For the adiabatic case, it is the total potential energy difference that has been found to correlate well with the total energy difference except for ethane whose rotation barrier is dominated by the quantum effect. © 2008 American Institute of Physics. [DOI: 10.1063/1.2976767]

I. INTRODUCTION

An unambiguous understanding of the origin of internal rotational barriers¹⁻³ is vital in our knowledge to fathom molecular conformational changes, which are closely related to fundamentally important problems in chemistry and biology such as protein folding and misfolding⁴ (involved in mad cow disease, Parkinson disease, Alzheimer disease, etc.), signal transduction cascades^{5,6} in cells, as well as chemical reactivity for individual molecules (regio-, diastereo-, and enantioselectivity). However, the current status on the matter is far from clear; even for the simplest system of ethane there exists no consensus in the literature on the origin of its internal rotational barrier.⁷⁻¹⁶ The main controversy lies in attributing different amounts of steric, electrostatic, and hyper-

conjugation (quantum) effects to the barrier height. The following two representative views are typical, one by Mulliken¹⁷ suggesting that the hyperconjugation plays the dominant role and the other by the intuitive, steric repulsion theory which dictates that the barrier originates from the steric repulsion.

This discrepancy of and disagreement in the interpretation, in our opinion, results from the equivocal definition of chemical concepts such as steric effect, which is known to be a *noumenon*,¹⁸ an object of human inquiry, understanding, or cognition, for which there is no unique quantification, in contrast to any physically observable *phenomenon*. The steric effect, which originates from the fact that atoms in molecules (AIMs) occupy a certain amount of space and when atoms are brought together, hindrance will be necessarily induced, resulting in changes in shape, energy, and reactivity, is an essential and universal concept in chemistry, biochemistry, and pharmacology, affecting rates and energies of chemical reactions, impacting structure, dynamics, and function of en-

^{a)}Authors to whom correspondence should be addressed.

^{b)}Electronic mail: shubin@email.unc.edu.

^{c)}Electronic mail: lee_pedersen@unc.edu.

zymes, and governing to a degree how and at what rate a drug molecule interacts with a receptor. However, there is no consensus in the literature on how to uniquely quantify this effect. Earlier, Weisskopf¹⁹ attributed it to the “kinetic energy pressure” in atoms and molecules, whereas others^{7–9,11,20,21} employed the quantum contribution from the Pauli exclusion principle (Fermi hole)^{22–26} for the purpose. Different algorithms and disparate implementations using orthogonal/nonorthogonal localized/delocalized orbitals, natural bond orbitals (NBOs), and valence bond orbitals lead to subtle but variant explanations and thus ongoing controversy on the matter.

It is our belief that the steric effect is an intrinsic property of atoms and molecules. On the other hand, if the effect relates to the shape an atom or molecule takes or space it occupies, one needs to make clear that other effects such as quantum and electrostatic effects also contribute to the constitution of an atomic or molecular framework. The contribution from the quantum effect prevents both same-spin (Fermi hole) and opposite-spin (Coulomb hole) electrons from coming together, whereas the contribution from electrostatic interactions such as classical electron-electron and nuclear-nuclear Coulomb repulsions also keeps both electrons and nuclei in a molecule in balance and thus contribute to the composition of the atomic or molecular scaffold as well. It is important that one distinguishes these effects from the steric effect when the latter is quantified. Other desirable properties of an acceptable quantification of the steric effect are that it is repulsive and extensive. The repulsiveness property is required by the hindrance nature of the effect and the extensiveness feature is to reflect that the bulkier the system, the larger the steric effect. Another consideration is that quantifications of the effect in the literature thus far are all orbital based. Is there a density-based description of the effect?

Recently, a density-based quantification of the steric and quantum effects has been proposed.²⁷ Within the new energy partition scheme under the framework of density functional theory (DFT),²⁸ the total energy density functional is decomposed into three independent contributions from steric, electrostatic, and quantum effects. Appealing properties of the new definition have been revealed and its intrinsic relation to Bader’s²⁹ AIM approach has been unveiled. It has also been applied to ethane and *n*-butane to examine the internal rotation barriers.³⁰ In this work, we continue our endeavor, applying to the category of carbon, nitrogen, and oxygen containing molecules that have only one rotatable dihedral angle.³¹ Specifically, the following six compounds, CH₃CH₃ (ethane), CH₃NH₂ (methylamine), CH₃OH (methanol), NH₂NH₂ (hydrazine), NH₂OH (hydroxylamine), and H₂O₂ (hydrogen peroxide), with only one rotatable dihedral angle $\angle\text{H}-\text{X}-\text{Y}-\text{H}$ ($\text{X}, \text{Y}=\text{C}, \text{N}, \text{O}$), will be investigated. The list is systematic in the degree of involvement of classical lone pairs. The purpose of the present study is to apply the density-based approach to this simplest class of molecular systems.

Internal rotational barriers of these six molecules have been of considerable interest in the literature.^{31–33} Accurate estimates of their barrier height were available as early as 70

years ago.³⁴ They have also been extensively examined by various approaches. It is known that ethane, methylamine, and methanol each have two well-defined conformations, a less stable eclipsed state and a ground-state staggered isomer. For hydrazine, NH₂NH₂, the skew conformation has been found to be most stable with the $\angle\text{H}-\text{N}-\text{N}-\text{H}$ skew dihedral angle very close to 90°, and there are two other less stable isomers, cis and trans, where the two N–H bonds are eclipsed and maximally staggered, respectively. For hydroxylamine, NH₂OH, the trans conformer is most stable, then cis, and the skew conformer is most unstable with the $\angle\text{H}-\text{N}-\text{O}-\text{H}$ dihedral angle close to 15°. For hydrogen peroxide, H₂O₂, the skew conformer is most stable, with the $\angle\text{H}-\text{O}-\text{O}-\text{H}$ skew dihedral angle about 113°. Two other isomers, cis and trans, are also available but they are less stable.

II. THEORETICAL FRAMEWORK

In DFT,²⁸ the total electronic energy can conventionally be expressed as follows:

$$E[\rho] = T_S[\rho] + V_{\text{ne}}[\rho] + J[\rho] + E_{\text{xc}}[\rho], \quad (1)$$

where $T_S[\rho]$, $V_{\text{ne}}[\rho]$, $J[\rho]$, and $E_{\text{xc}}[\rho]$ stand for the noninteracting kinetic, nuclear-electron attraction, classical electron-electron Coulomb repulsion, and exchange-correlation energy density functionals, respectively. Two terms in Eq. (1), $V_{\text{ne}}[\rho]$ and $J[\rho]$, are of the electrostatic nature. Hence,

$$E_e[\rho] = V_{\text{ne}}[\rho] + J[\rho]. \quad (2)$$

When computing the total energy of the system, one needs to add another term to the electrostatic contribution, the nuclear-nuclear repulsion V_{nn} , which is also of electrostatic nature. Equation (1) then becomes

$$E[\rho] = T_S[\rho] + E_e[\rho] + E_{\text{xc}}[\rho]. \quad (3)$$

Recently, one of the authors proposed a new energy partition scheme in the following manner:²⁷

$$E[\rho] \equiv E_s[\rho] + E_e[\rho] + E_q[\rho], \quad (4)$$

where $E_s[\rho]$, $E_e[\rho]$, and $E_q[\rho]$ stand for the independent energy contributions for the steric, electrostatic, and quantum effects, respectively, which can be explicitly defined as

$$E_s[\rho] \equiv T_W[\rho] = \frac{1}{8} \int \frac{|\nabla \rho(\mathbf{r})|^2}{\rho(\mathbf{r})} d\mathbf{r}, \quad (5)$$

where $T_W[\rho]$ is the Weizsäcker kinetic energy,³⁵ and

$$E_q[\rho] = E_{\text{xc}}[\rho] + E_{\text{Pauli}}[\rho] = E_{\text{xc}}[\rho] + T_S[\rho] - T_W[\rho], \quad (6)$$

with the Pauli energy^{36–40}

$$E_{\text{Pauli}}[\rho] \equiv T_S[\rho] - T_W[\rho] \quad (7)$$

denoting the portion of the kinetic energy that embodies all the quantum effect from the antisymmetric requirement of the total wave function by the Pauli exclusion principle. Notice that there is also a kinetic counterpart of the dynamic correlation effect, $T_c[\rho]$, already embedded in $E_{\text{xc}}[\rho]$.^{41–43}

The reason that the Weizsäcker kinetic energy can be regarded as the measurement of steric effect within the DFT

framework is based on the introduction of the following hypothetical state. If assumed to be bosons, all electrons in the ground state would be in the same state and therefore the total energy of the conjectural state without considering the contributions from electrostatic and quantum effects would simply be $T_w[\rho]$. $E_s[\rho]$ represents the state for which the least possible space is withheld and thus is an intrinsic property of the system.

This quantification of the steric effect has the following appealing features: (i) It is consistent with the original Weiskopf attribution of the steric effect to the “kinetic energy pressure”¹⁹ because $T_w[\rho]$ itself is indeed a kinetic energy, exact for one electron systems. (ii) Its physical meaning is the above conjectured boson state for electrons and the steric effect is the kinetic energy of the presumptive state. (iii) The steric energy density in Eq. (5) is repulsive because the integrand is nowhere negative, extensive because $E_s[\rho]$ is homogeneous of degree 1 in density scaling,^{44–46} i.e., $E_s[\gamma\rho] = \gamma E_s[\rho]$ for $0 \leq \gamma \leq 1$, and exclusive because it is independent of other effects as hypothesized in Eq. (4). (iv) In the limit of a homogeneous electron gas where the density gradient vanishes, the steric contribution from Eq. (5) also disappears, indicating that there exists no steric repulsion in the homogeneous electron gas. (v) If Bader’s definition of the zero-flux boundary condition is adopted, for which the zero-flux surfaces S of the electron density $\rho(\mathbf{r})$ are defined as the set of points \mathbf{r} obeying

$$\nabla\rho(\mathbf{r}) \cdot \mathbf{n}(\mathbf{r}) = 0, \quad \forall \mathbf{r} \in S, \quad (8)$$

and $\mathbf{n}(\mathbf{r})$ is the unit vector perpendicular to S at \mathbf{r} , the concept of AIM can then be established with the characteristic that they are interfaced with each other with the vanished steric energy density, exhibiting that AIMS acquire balanced steric repulsion among one another. (vi) Finally, because of the intrinsic relationship of this quantification to Bader’s AIM approach, we can accurately quantify contributions of the steric effect at three distinctive levels of structural partition: atomic, fragment, and molecular levels.

The potential associated with each of the three exclusive energy contributions, steric, electrostatic, and quantum, can be respectively defined as the functional derivative of the energy component with respect to the total electron density. For example, for the quantum contribution, which is also called the fermionic quantum energy^{47,48} because we use the boson state as reference, one can define the quantum potential $v_q(\mathbf{r})$,

$$v_q(\mathbf{r}) = \frac{\delta E_q[\rho]}{\delta \rho(\mathbf{r})} = \mu - v_{\text{ext}}(\mathbf{r}) - v_f(\mathbf{r}) - v_s(\mathbf{r}), \quad (9)$$

where $v_{\text{ext}}(\mathbf{r})$, $v_f(\mathbf{r})$, and $v_s(\mathbf{r})$ denote the functional derivative of $V_{\text{ne}}[\rho]$, $J[\rho]$, and $E_s[\rho]$, respectively, with

$$v_f(\mathbf{r}) = \int \frac{\rho(\mathbf{r}')}{|\mathbf{r} - \mathbf{r}'|} d\tau' \quad (10)$$

and

$$v_s(\mathbf{r}) = \frac{\delta E_s[\rho]}{\delta \rho(\mathbf{r})} = \frac{1}{8} \frac{|\nabla\rho(\mathbf{r})|^2}{\rho(\mathbf{r})} - \frac{1}{4} \frac{\nabla^2\rho(\mathbf{r})}{\rho(\mathbf{r})}. \quad (11)$$

Notice that all quantities on the right-hand side of Eq. (9) are explicitly known and no exchange-correlation potential is involved in the fermionic quantum potential defined in this manner. The quantum charge $q_q(\mathbf{r})$ can be defined as follows:⁴⁹

$$\nabla^2 v_q(\mathbf{r}) = -4\pi q_q(\mathbf{r}). \quad (12)$$

Again, these quantities can be defined at the atomic, group, or molecular level with the adoption of the AIM criterion, Eq. (8).

We reiterate that the new decomposition, Eq. (4), is an assumption using the Weizsäcker kinetic energy as the reference representing a hypothetical state where electrons are conjectured to be bosons. Also, there are other equivalent ways to express $T_w[\rho]$ for atoms and molecules since⁵⁰

$$\begin{aligned} T_w[\rho] &= \frac{1}{8} \int \frac{|\nabla\rho(\mathbf{r})|^2}{\rho(\mathbf{r})} d\mathbf{r} = \frac{1}{8} \int \frac{\nabla\rho(\mathbf{r}) \cdot \nabla\rho(\mathbf{r})}{\rho(\mathbf{r})} d\mathbf{r} \\ &= \frac{1}{8} \int \nabla\rho(\mathbf{r}) \cdot \nabla \ln \rho(\mathbf{r}) d\mathbf{r} \\ &= -\frac{1}{8} \int \nabla^2\rho(\mathbf{r}) \ln \rho(\mathbf{r}) d\mathbf{r}, \end{aligned} \quad (13)$$

confirming that as a noumenon, the steric effect has no unique quantification even within the framework of DFT. We mention in passing that $T_w[\rho]$ is closely associated with the so-called Fisher information and so the above identities in Eq. (13) also provide alternative expressions for the Fisher information for atoms and molecules.^{47,48,50}

Now, applying the above energy partition schemes to conformation changes, we are interested in calculating the total energy difference between any two conformations of a rotatable molecule and then analyzing the contribution from different energy components in different partition schemes. With the conventional DFT total energy formula, Eq. (3), one has

$$\Delta E[\rho] = \Delta T_s[\rho] + \Delta E_e[\rho] + \Delta E_{\text{xc}}[\rho], \quad (14)$$

whereas from Eq. (4) there results

$$\Delta E[\rho] = \Delta E_s[\rho] + \Delta E_e[\rho] + \Delta E_q[\rho]. \quad (15)$$

One of the main purposes of this and many other studies in the literature on the origin of internal rotational barrier is to ascertain if there is one quantity from the above equations dictating the rotation barrier height ΔE during the course of internal conformation changes. Similar endeavors are found elsewhere.^{51–56}

In a recent work³⁰ we applied Eq. (15) to ethane and unveiled that the eclipsed conformer does possess a larger steric repulsion than the staggered conformer, in accordance with chemical intuition. On the other hand, we also observed that there exists an excellent linear relationship for both fixed and relaxed geometries between the total energy change ΔE and the fermionic quantum energy difference ΔE_q , $\Delta E_q \sim \Delta E$, along the course of the $\angle\text{H-C-C-H}$ dihedral angle

TABLE I. Adiabatic differences of the total energy and various energy components between different conformations for the six molecular systems. Structures have been optimized at the B3LYP/aug-cc-pvDZ level of theory. Units are in kcal/mol.

Adiabatic difference	ΔE	ΔE_s	ΔE_q	ΔE_e	ΔT_s	ΔE_{xc}	$\Delta(\text{NBOSteric})$
C ₂ H ₆ eclipsed–staggered	2.75	4.43	−4.24	2.56	−1.23	1.41	−7.97
CH ₃ NH ₂ eclipsed–staggered	1.93	−8.87	6.44	4.36	−2.56	0.13	1.14
CH ₃ OH eclipsed–staggered	1.04	−2.61	1.34	2.31	−1.36	0.09	−0.66
NH ₂ NH ₂ trans–skew	2.75	87.20	−78.17	−6.27	−0.15	9.17	12.28
NH ₂ NH ₂ cis–trans	5.79	−4.11	−0.30	10.20	−6.44	2.03	−19.50
NH ₂ NH ₂ cis–skew	8.54	83.09	−78.47	3.93	−6.59	11.21	−7.22
NH ₂ OH cis–trans	2.59	30.12	−28.41	0.90	−2.29	4.00	0.89
NH ₂ OH skew–cis	4.28	7.83	−10.30	6.74	−4.55	2.08	−9.10
NH ₂ OH skew–trans	6.87	37.95	−38.71	7.64	−6.84	6.08	−8.21
H ₂ O ₂ trans–skew	0.98	3.92	−1.50	−1.42	2.29	0.13	−0.91
H ₂ O ₂ cis–trans	6.29	28.40	−29.74	7.63	−6.08	4.74	−6.93
H ₂ O ₂ cis–skew	7.27	32.32	−31.24	6.20	−3.79	4.87	−7.84

rotation, indicating that the rotation barrier is indeed of quantum nature, governed by the fermionic quantum effect. This relationship, however, was found to be absent for *n*-butane, revealing that the relationship is not universal and that the matter is complex and subtle. In this work, we extend the study to molecules such as CH₃CH₃ (ethane), CH₃NH₂ (methylamine), CH₃OH (methanol), NH₂NH₂ (hydrazine), NH₂OH (hydroxylamine), and H₂O₂ (hydrogen peroxide) for which there exists only one available intramolecular dihedral angle³¹ and examine the nature of energy component contributions in both the conventional and new energy partition schemes.

We emphasize that we are here concerned with the contributions of the effects at the molecular level only. Results at the atomic level (e.g., atoms C, N, or O) or group/fragment level (e.g., −CH₃, −NH₂, or −OH) via Bader's AIM definition of atoms and groups will be presented elsewhere.

III. COMPUTATIONAL METHODS

Two kinds of rotational barrier heights will be considered and examined in this study, adiabatic (i.e., with optimized geometry) and vertical (i.e., with fixed geometry).^{55–59} In the adiabatic dihedral angle rotation, both staggered and eclipsed conformers are in their respective optimized structure, whereas in the vertical case, bond lengths and angles for the two conformers are fixed to be identical except for the changing dihedral angle. For the adiabatic rotation, each time the dihedral angle of the two conformers is altered, a geometrical optimization with that dihedral angle will be performed. For the vertical category, we employ the optimized geometry of the staggered (most stable) conformer as the starting structure and the eclipsed conformer is obtained from the starting structure by changing the dihedral angle from 180° to 0°. No structural optimization is carried out. The dihedral angle considered for ethane is ∠H–C–C–H, for methylamine ∠H–C–N–H, for methanol ∠H–C–O–H, for hydrazine ∠H–N–N–H, for hydroxylamine ∠H–N–O–H, and for hydrogen peroxide ∠H–O–O–H. The dihedral angle change range is from 0° to 360° with the interval of 5°. For each of CH₃CH₃, CH₃NH₂, and CH₃OH there is only one difference, eclipsed–staggered ($\Delta E > 0$), but for NH₂NH₂, NH₂OH, and

H₂O₂ three differences are possible for each system. We define the difference so that ΔE is always greater than zero. To that end, we always choose the more stable state as the reference. We will make two profiles, adiabatic and vertical, of the total energy and energy component differences for all six molecules as a function of the dihedral angle from 0° to 360°. To do that, we always use the most stable conformation for each system as the reference, whose dihedral angle is set to be zero.

The above formulations have been implemented in the NWChem (Ref. 60) suite of software, a publicly accessible, computational chemistry package from Pacific Northwest National Laboratory that is designed to run on high-performance parallel supercomputers and clusters. We used the hybrid B3LYP (Refs. 61 and 62) functional and Dunning's⁶³ aug-cc-pVDZ basis set. The tight self-consistent field convergence criterion and ultrafine integration grids are employed throughout.

As is well known, an alternative description of the steric effect in terms of the Pauli exclusion principle (Fermi hole) has been available in the literature.^{7–9,11,20,21} As a comparison, we also calculated the steric energy from this quantification using NBOs for all the systems. The NBOFILE keyword in NWChem was used to create an input file to be used as the input for the stand-alone NBO analysis code, NBO, version 5.0.⁶⁴ We term the result from this calculation as the NBO steric energy thereafter with the difference denoted by $\Delta\text{NBOSteric}$.

IV. RESULTS AND DISCUSSION

Let us consider distinctive isomers of the six systems first. We know that for ethane, methylamine, and methanol each has two conformations, *staggered* and *eclipsed*, whereas for hydrazine, hydroxylamine, and hydrogen peroxide each molecule has three different isomers, *cis*, *trans*, and *skew*, with varying stability orders. The most stable conformer of hydrazine, hydroxylamine, and hydrogen peroxide was found to be skew, *trans*, and skew, respectively. Table I shows the adiabatic total energy difference and its five energy components from Eqs. (14) and (15) for these species. The internal rotation barriers computed for these species shown in Table I are consistent with other theoretical

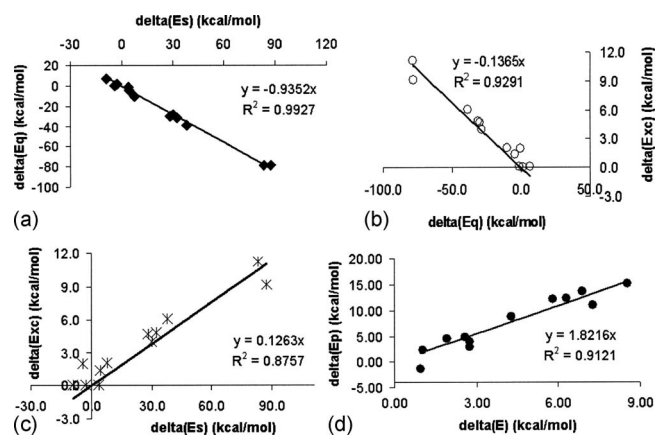


FIG. 1. Observed linear relationships and their correlation coefficients among different energy components in different energy partition schemes for the adiabatic structures of the six molecular systems from this study: (a) $\Delta E_s \sim \Delta E_q$, $R^2=0.9927$; (b) $\Delta E_q \sim \Delta E_{xc}$, $R^2=0.9291$; (c) $\Delta E_s \sim \Delta E_{xc}$, $R^2=0.8757$; and (d) $\Delta E \sim \Delta E_p$, $R^2=0.9121$.

studies^{7,11,32} and experimental results.^{65,66} For the comparison purpose, the steric energy from the NBO analysis is also shown in the table. It can be found that given $\Delta E > 0$, none of the six energy components in Eqs. (14) and (15) is always positive, suggesting that none of them is the dominant factor making $\Delta E > 0$. Also, $\Delta E_s > 0$ except for three cases, CH_3NH_2 , CH_3OH , and the cis/trans difference in NH_2NH_2 , indicating that in a majority of situations the steric repulsion in a less stable conformation is larger than the more stable state, so steric repulsion does positively contribute to the rotational barrier height. On the other hand, the steric energy difference from the NBO analysis (last column of the table) is negative except for three cases, demonstrating that in a majority of situations, in contrast to the traditional chemical intuition, a more stable isomer has a larger NBO steric repulsion.

When a molecule is in the equilibrium state, virial theorem ensures certain linear relationships between the total energy and some of the energy components. However, when the system is away from the equilibrium, a more complicated relationship holds.^{52–56} For energy differences, these relationships may or may not be valid. Does there exist any linear relationship among the quantities of different molecules listed in Table I? Figure 1 exhibits the four most correlated relationships discovered, where we find that ΔE_s , ΔE_q , and ΔE_{xc} are intercorrelated with each other with the correlation coefficient R^2 between $\Delta E_s \sim \Delta E_q$ [Fig. 1(a)], $\Delta E_q \sim \Delta E_{xc}$ [Fig. 1(b)], and $\Delta E_s \sim \Delta E_{xc}$ [Fig. 1(c)] equal to 0.9927, 0.9291, and 0.8757, respectively. In addition, we observed a little weaker correlation between ΔE_e and $\Delta \text{NBOSteric}$ with $R^2=0.7677$ (not shown). What do these relations tell us? The existence of strong correlations between energy component differences during the course of conformation changes suggests that changes in different effects are compensated and interdependent—when one effect is changed, so are the rest. We notice that there is no significant correlation between the total adiabatic energy difference ΔE and any of the energy component differences from Eqs. (14) and (15) in the table, indicating that when all adiabatic differences for these sys-

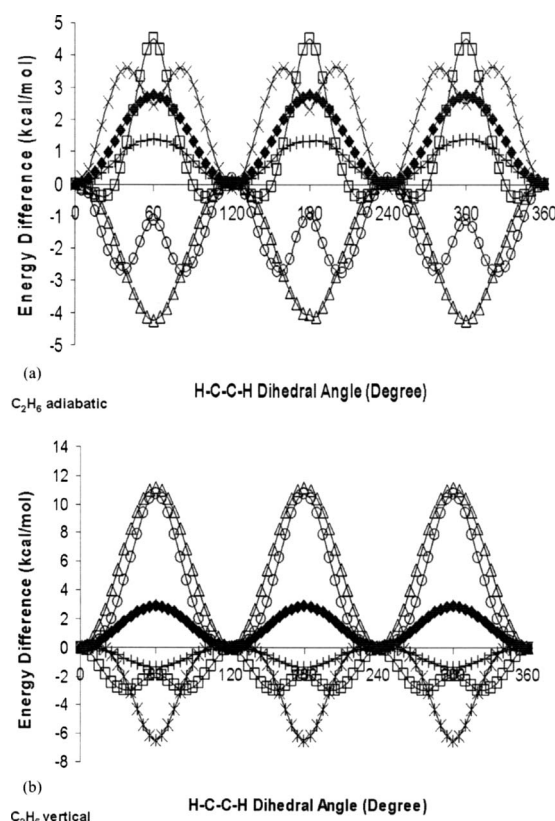


FIG. 2. (a) Adiabatic and (b) vertical energy differences of various energy components from different energy partition schemes for ethane, CH_3CH_3 , as a function of the $\angle \text{H-C-C-H}$ dihedral angle. Solid diamond: ΔE ; square: ΔE_s ; triangle: ΔE_q ; star: ΔE_e ; circle: ΔT_s ; plus: ΔE_{xc} .

tems are put together, there is no single component dictating the rotation barrier. However, as is shown in Fig. 1(d), if we rewrite Eq. (14) as

$$\Delta E[\rho] = \Delta T_s[\rho] + \Delta E_p[\rho], \quad (16)$$

where $E_p[\rho]$ stands for the sum of the contributions from the potential energies,

$$\Delta E_p[\rho] = \Delta E_e[\rho] + \Delta E_{xc}[\rho], \quad (17)$$

a reasonably linear relationship [Fig. 1(d)] between ΔE and ΔE_p is observed with $R^2=0.9121$. No significant correlation between ΔE and ΔT_s in Eq. (17) or between ΔE and the sum of any pair of the three terms in Eq. (15) is found.

Figures 2–7 display the adiabatic (a) and vertical (b) energy difference profiles as a function of the $\angle \text{H-X-Y-H}$ ($X, Y = \text{C, N, O}$) dihedral angle change from 0° to 360° . Again, in the adiabatic (relaxed-geometry) case, structures are fully optimized except for the changing dihedral angle, whereas in the vertical (fixed-geometry) case we take bond lengths and angles of the staggered conformer, and for the convenience of comparison we reset the value of the most stable structure to be the origin so that $\Delta E > 0$. A second vertical case is possible where one takes the bond lengths and angles from the eclipsed isomer but our recent study shows that the two vertical results are qualitatively identical.

In the adiabatic profile for ethane [Fig. 2(a)], ΔE_s , ΔE_e , and ΔE_{xc} are positive (except for a few points close to the staggered isomer for ΔE_s) and ΔE_q and ΔT_s are always nega-

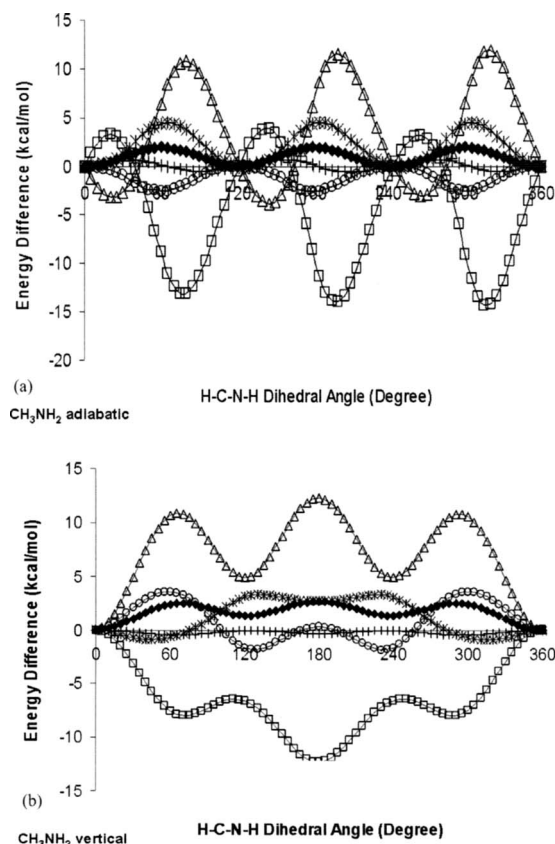


FIG. 3. (a) Adiabatic and (b) vertical energy differences of various energy components from different energy partition schemes for methylamine, CH_3NH_2 , as a function of the $\angle\text{H-C-N-H}$ dihedral angle. Solid diamond: ΔE ; square: ΔE_s ; triangle: ΔE_q ; star: ΔE_e ; circle: ΔT_s ; plus: ΔE_{xc} .

itive, illustrating that ΔE_s , ΔE_e , and ΔE_{xc} contribute positively to ΔE whereas ΔE_q and ΔT_s contribute negatively. In the vertical case [Fig. 2(b)], however, their roles are completely reversed with ΔE_q and ΔT_s being positive and ΔE_s , ΔE_e , and ΔE_{xc} negative, implying that from the energy component perspective, internal dihedral angle rotations with and without geometry relaxation are different in nature. It is because, as can be seen in Table I, changes in structures (bond distances and angles) and effects have to be compensated, so structure changes with relaxation are different from those without. Whether or not a completely different scenario is seen in the two cases depends on the chemical composition of the system.

For the adiabatic case of CH_3NH_2 [Fig. 3(a)], ΔE_e and ΔT_s are positively and negatively contributed, respectively, at the entire range of internal rotation, whereas the other components, ΔE_s , ΔE_q , and ΔE_{xc} , change their sign as the dihedral angle increases. In the vertical case [Fig. 3(b)], however, one finds that ΔE_q and ΔE_s are always positive and negative, respectively, but the others, ΔE_e , ΔT_s , and ΔE_{xc} , change their sign during the rotation. These results confirm what has been seen in C_2H_6 that relaxed- and fixed-geometry results are substantially different. For methanol, shown in Fig. 4, the results are a little different, where it is observed that in both cases ΔE_q and ΔE_e always contribute positively and ΔE_s negatively, the contribution from ΔE_{xc} is negligible, and it is only the ΔT_s term that changes sign. Quantitatively,

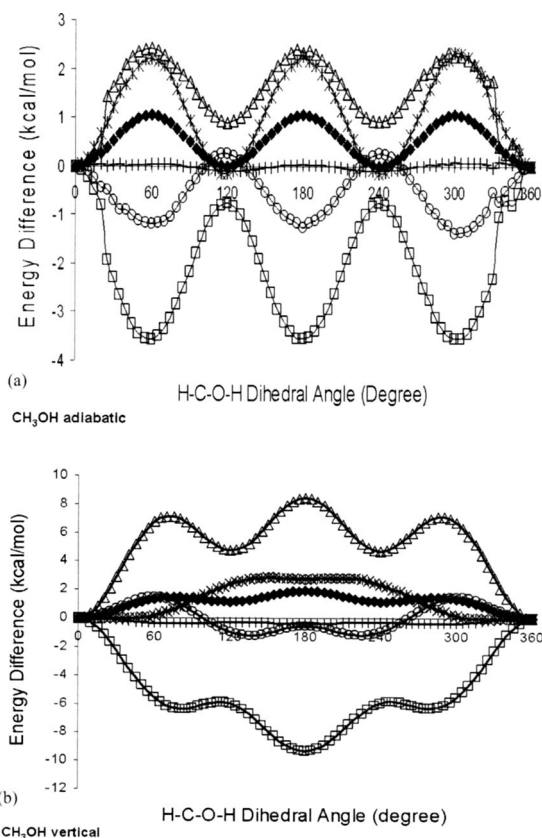


FIG. 4. (a) Adiabatic and (b) vertical energy differences of various energy components from different energy partition schemes for methanol, CH_3OH , as a function of the $\angle\text{H-C-O-H}$ dihedral angle. Solid diamond: ΔE ; square: ΔE_s ; triangle: ΔE_q ; star: ΔE_e ; circle: ΔT_s ; plus: ΔE_{xc} .

however, both their value and profile shape for the adiabatic and vertical differences are noticeably different. We note that ΔE_s are negative in both cases for both CH_3NH_2 and CH_3OH .

In the adiabatic case for hydrazine [Fig. 5(a)], we find strong polarization (large values with different signs) between ΔE_s and ΔE_q with ΔE_s contributing positively and ΔE_q negatively. The polarization becomes smaller in the vertical case but the profile shape becomes more complicated than that of the adiabatic case. Similar strong polarization between ΔE_s and ΔE_q is also found for hydroxylamine and hydrogen peroxide [Figs. 6(a) and 7(a)]. Compared to ethane, methylamine, and methanol, where no such effect is visible, it can be attributed to the existence of lone pair(s) in the systems, suggesting that contributions from the lone pair(s) to ΔE_s and ΔE_q can be larger. In Fig. 6(a), we see the first example without a sign change, as ΔE_s , ΔE_e , and ΔE_{xc} are always positive and ΔE_q and ΔT_s negative. Again, its vertical counterpart [Fig. 6(b)] is drastically different, especially the steric energy component ΔE_s . Similar tendencies are shown in Fig. 7 although its second peak [in Fig. 7(a)] is considerably smaller than the first. Notice that for the adiabatic case of NH_2NH_2 , NH_2OH , and H_2O_2 , ΔE_s is always larger than zero, illustrating that steric repulsion serves as the positive factor contributing to $\Delta E > 0$.

As comparison to ΔE_s , shown in Fig. 8 are the adiabatic [Fig. 8(a)] and vertical [Fig. 8(b)] $\Delta\text{NBOSteric}$ profiles with respect to the dihedral change for all six systems. No appar-

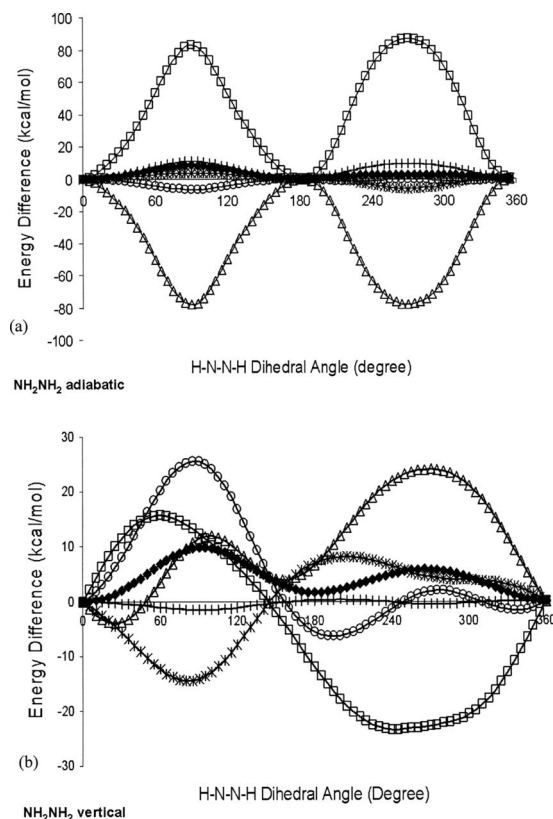


FIG. 5. (a) Adiabatic and (b) vertical energy differences of various energy components from different energy partition schemes for hydrazine, NH_2NH_2 , as a function of the $\angle\text{H-N-N-H}$ dihedral angle. Solid diamond: ΔE ; square: ΔE_s ; triangle: ΔE_q ; star: ΔE_e ; circle: ΔT_s ; plus: ΔE_{xc} .

ent pattern of change is seen, but one finds that in the adiabatic case [Fig. 8(a)] except for hydrazine, the majority of $\Delta\text{NBOSteric}$ is less than zero. This is consistent with the results from Table I, where $\Delta\text{NBOSteric}$ was found to contribute negatively to ΔE except for three cases. In the vertical case [Fig. 8(b)], however, the situation is reversed, with more systems giving $\Delta\text{NBOSteric} > 0$, confirming what has been observed in Figs. 1–7 that adiabatic and vertical cases tend to yield significantly different results. It has been indicated by Badenhop and Weinhold⁶⁷ that this counterintuitive exchange-favored eclipsing effect results from the highly favored “delocalization energy” due to hyperconjugation in the staggered conformation.

To examine whether or not there exist strong correlations among the total energy and energy component differences as shown in Fig. 1, we carried out the linear regression analysis for all possible combinations of all quantities in Eqs. (14) and (15) for both adiabatic and vertical differences with the total number of the data points of 73 in each fit. We also considered all possible combinations, Eq. (16) as an example, of the sum of two quantities at the right-hand side of Eqs. (14) and (15). In principle, if one energy component difference in either Eq. (14) or Eq. (15) correlate well with the total energy difference, so does the sum of the remaining two terms. For example, if there is a strong correlation between ΔE_{xc} and ΔE , from Eq. (14) a similarly good linear relationship between $\Delta T_s + \Delta E_e$ and ΔE is anticipated. However, the reverse may not be true. The exception, as will be

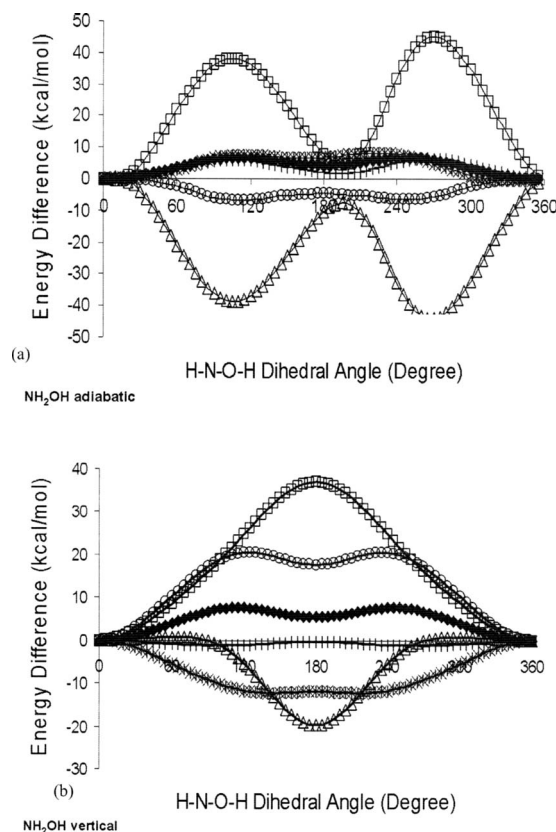


FIG. 6. (a) Adiabatic and (b) vertical energy differences of various energy components from different energy partition schemes for hydroxylamine, NH_2OH , as a function of the $\angle\text{H-N-O-H}$ dihedral angle. Solid diamond: ΔE ; square: ΔE_s ; triangle: ΔE_q ; star: ΔE_e ; circle: ΔT_s ; plus: ΔE_{xc} .

shown below, is when the sum of the two quantities is dominantly larger in magnitude than the remaining component.

Table II shows the discovered strong relationships ($R^2 > 0.9$) and their correlation coefficients. Overall, we did not find a universal linear relationship between ΔE and any energy component for both relaxed and fixed geometries, implying that at least for these systems there is no universal energy component from the two energy partition schemes [Eqs. (14) and (15)] governing the rotation barrier height for all of the molecules. However, using the sum of the two components from Eq. (14), we find that the linear relationship between ΔE and $\Delta T_s + \Delta E_e$ applies to the vertical (fixed structure) difference of all the six systems and $\Delta E \sim \Delta E_{xc} + \Delta E_e$ is valid for all adiabatic (relaxed structure) cases except ethane, confirming once again that origins of rotational barrier heights for fixed and relaxed geometries are different in nature. We note that ethane is the only molecule in this study with no lone pair. The correlation coefficient between ΔE and $\Delta E_{xc} + \Delta E_e$ for ethane is 0.7487, a much weaker correlation than what has been found in other systems. The almost universal relationship between ΔE and $\Delta E_{xc} + \Delta E_e$ for the adiabatic case is consistent with the result in Fig. 1(d).

For ethane, confirming what was discovered earlier,³⁰ a linear relationship between ΔE and ΔE_q (and thus $\Delta E_s + \Delta E_e$) is seen for both adiabatic and vertical cases. A similar relationship is also present in the vertical case for CH_3NH_2 and CH_3OH . For the adiabatic case of C_2H_6 , we also found strong correlations between ΔE and ΔE_{xc} (and thus ΔT_s

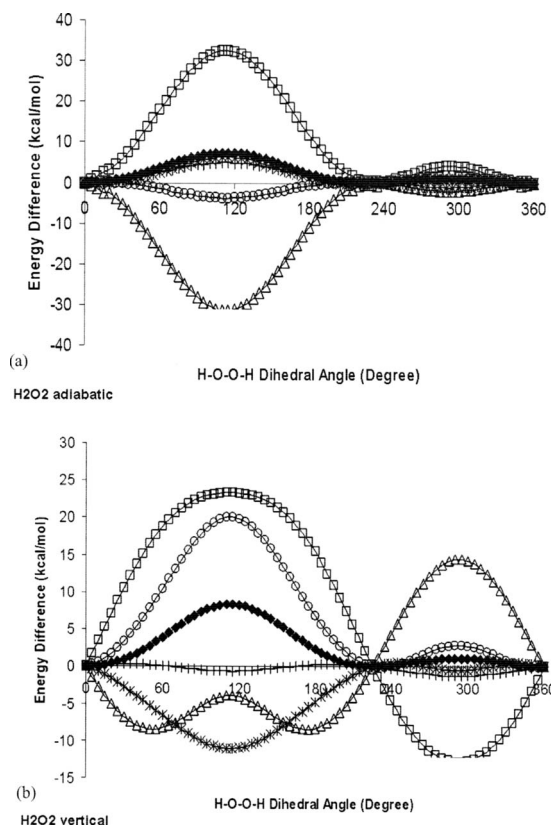


FIG. 7. (a) Adiabatic and (b) vertical energy differences of various energy components from different energy partition schemes for hydrogen peroxide, H_2O_2 , as a function of the $\angle\text{H-O-O-H}$ dihedral angle. Solid diamond: ΔE ; square: ΔE_s ; triangle: ΔE_q ; star: ΔE_e ; circle: ΔT_s ; plus: ΔE_{xc} .

+ ΔE_e), giving $R^2=0.9961$ for $\Delta E \sim \Delta E_{xc}$ and $R^2=0.9954$ for $\Delta E_{xc} \sim \Delta T_s + \Delta E_e$. Correlation is seen between ΔE_{xc} and ΔE_q with $R^2=0.9815$. More linear relationships are found in the vertical case of ethane, where ΔE , ΔE_q , ΔE_{xc} , and $\Delta\text{NBOSteric}$ are found to be strongly intercorrelated. It is one of the two cases where $\Delta\text{NBOSteric}$ is found to be strongly correlated with ΔE ($\Delta E=0.9934 \times \Delta\text{NBOSteric}$, $R^2=0.9992$). For both adiabatic and vertical cases of ethane, ΔE is dedicated by ΔE_q or ΔE_{xc} , meaning that the internal rotation barrier originates from the quantum effect.

For CH_3NH_2 , two linear relationships, $\Delta E \sim \Delta T_s$ (and thus $\Delta E_{xc} + \Delta E_e$) and $\Delta E_q \sim \Delta E_s$ for the adiabatic case and $\Delta E \sim \Delta E_q$ (thus $\Delta E_s + \Delta E_e$) and $\Delta E \sim \Delta T_s + \Delta E_e$ for the vertical case, are discovered. Notice that no strong correlation between ΔE and ΔE_{xc} is seen for the vertical case owing to the exception reason mentioned above. In the CH_3OH adiabatic case, ΔE is seen to be strongly correlated with both ΔT_s and ΔE_e because ΔT_s and ΔE_e are linearly correlated with the correlation coefficient $R^2=0.9663$. For the vertical case, however, we find that ΔE linearly correlates well with ΔE_s ($R^2=0.9656$), ΔE_q ($R^2=0.9693$), and $\Delta T_s + \Delta E_e$ ($R^2=0.9969$). We also observed a little weaker correlation between ΔE_q and ΔE_{xc} .

In the adiabatic case of hydrazine, ΔE_s , ΔE_q , and ΔE_{xc} are found to be strongly correlated with each other. The total energy difference ΔE is found to correlate well with $\Delta E_{xc} + \Delta E_e$ and a little weaker with ΔT_s . In the vertical case, these linear relationships disappear and, again, $\Delta E \sim \Delta T_s + \Delta E_e$

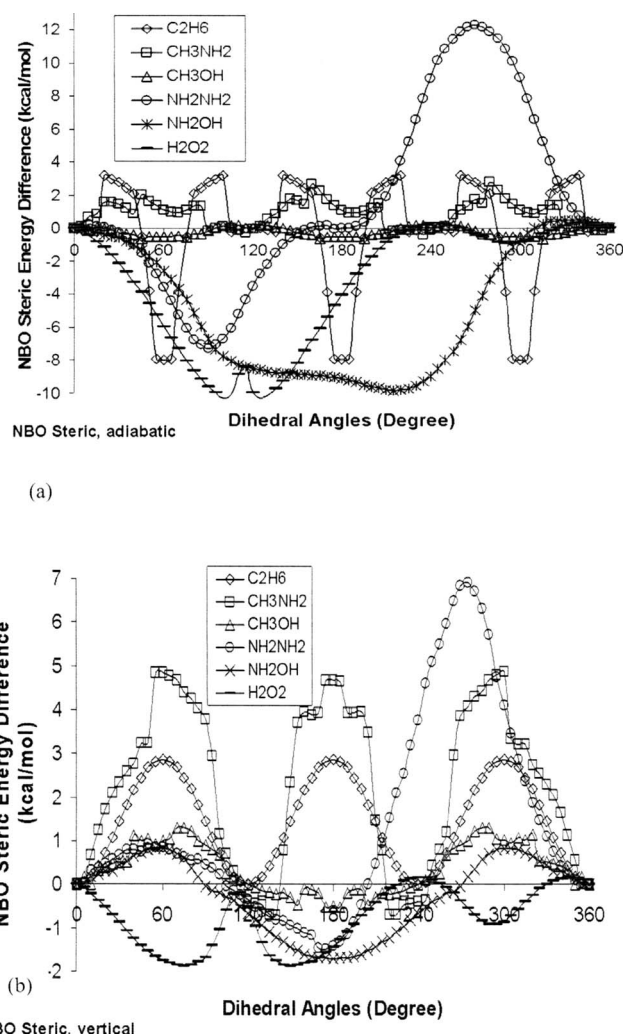


FIG. 8. (a) Adiabatic and (b) vertical NBO steric energy differences from the NBO 5.0 analysis for CH_3CH_3 , CH_3NH_2 , CH_3OH , NH_2NH_2 , NH_2OH , and H_2O_2 as a function of the $\angle\text{H-X-Y-H}$ ($X, Y=\text{C, N, O}$) dihedral angle.

with $R^2=0.9893$ plus a weak correlation between ΔE_{xc} and ΔT_s with $R^2=0.9208$ is ascertained. For NH_2OH , ΔE_q , ΔE_s , and ΔE_{xc} are found to be intercorrelated in the adiabatic difference, so are ΔE , ΔT_s , and ΔE_e in the vertical case. More linear relationships have been unveiled for the adiabatic H_2O_2 case, where five quantities, ΔE , ΔE_s , ΔE_q , ΔE_{xc} , and $\Delta\text{NBOSteric}$, are observed to be interdependent. We find the second example where the total energy difference (barrier height) ΔE is linearly correlated with the steric energy difference ΔE_s ($R^2=0.9915$), where we also see the second incidence that ΔE is proportional to $\Delta\text{NBOSteric}$ ($R^2=0.9665$). In the vertical case, fewer relationships are found except for the interdependence among ΔE , ΔT_s , and ΔE_e . Again, we observe strong correlations of $\Delta E \sim \Delta E_{xc} + \Delta E_e$ in the adiabatic case and $\Delta E \sim \Delta T_s + \Delta E_e$ in the vertical difference.

Overall, we have not observed a universal linear relationship between ΔE and any of the energy components that may be applicable to all the systems. However, for the relaxed-geometry (adiabatic) difference, we find the strong relationship between ΔE and $\Delta E_{xc} + \Delta E_e$ except for ethane and in the fixed-geometry (vertical) case a strong correlation

TABLE II. Strong ($R^2 > 0.9$) linear relationships and their correlation coefficients among the various energy component differences for both the optimal (adiabatic) and fixed (vertical) structures for the six molecular systems in the present investigation.

	Adiabatic (relaxed geometry)		Vertical (fixed geometry)	
	Strong correlations	R^2	Strong correlations	R^2
C_2H_6	$\Delta E \sim \Delta E_q$	0.9899	$\Delta E \sim \Delta E_q$	0.9998
	$\Delta E \sim \Delta E_{xc}$	0.9961	$\Delta E \sim \Delta E_{xc}$	0.9879
	$\Delta E \sim \Delta T_s + \Delta E_e$	0.9954	$\Delta E \sim \Delta E_s + \Delta E_e$	0.9996
	$\Delta E \sim \Delta E_s + \Delta E_e$	0.9959	$\Delta E \sim \Delta T_s + \Delta E_e$	0.9986
	$\Delta E_q \sim \Delta E_{xc}$	0.9815	$\Delta E \sim \Delta NBO_{Steric}$	0.9991
CH_3NH_2			$\Delta E_q \sim \Delta E_{xc}$	0.9908
			$\Delta E_{xc} \sim \Delta NBO_{Steric}$	0.9845
			$\Delta E_q \sim \Delta NBO_{Steric}$	0.9992
	$\Delta E \sim \Delta T_s$	0.9781	$\Delta E \sim \Delta E_q$	0.9797
	$\Delta E \sim \Delta E_{xc} + \Delta E_e$	0.9924	$\Delta E \sim \Delta T_s + \Delta E_e$	0.9891
CH_3OH	$\Delta E_s \sim \Delta E_q$	0.9857	$\Delta E \sim \Delta E_s + \Delta E_e$	0.9661
	$\Delta E \sim \Delta E_e$	0.9874	$\Delta E \sim \Delta E_q$	0.9693
	$\Delta E \sim \Delta T_s$	0.9209	$\Delta E \sim \Delta E_s$	0.9656
	$\Delta E \sim \Delta T_s + \Delta E_e$	0.9774	$\Delta E \sim \Delta T_s + \Delta E_e$	0.9969
	$\Delta E \sim \Delta E_s + \Delta E_q$	0.9608	$\Delta E \sim \Delta E_q + \Delta E_e$	0.9761
NH_2NH_2	$\Delta T_s \sim \Delta E_e$	0.9663	$\Delta E \sim \Delta E_s + \Delta E_e$	0.9485
			$\Delta E_q \sim \Delta E_{xc}$	0.9245
	$\Delta E \sim \Delta T_s$	0.9015	$\Delta E \sim \Delta T_s + \Delta E_e$	0.9893
	$\Delta E \sim \Delta E_{xc} + \Delta E_e$	0.9806	$\Delta E_{xc} \sim \Delta T_s$	0.9208
	$\Delta E_q \sim \Delta E_s$	0.9980		
NH_2OH	$\Delta E_q \sim \Delta E_{xc}$	0.9717		
	$\Delta E_s \sim \Delta E_{xc}$	0.9580		
	$\Delta E \sim \Delta E_{xc} + \Delta E_e$	0.9875	$\Delta E \sim \Delta T_s$	0.9735
	$\Delta E_q \sim \Delta E_s$	0.9881	$\Delta E \sim \Delta E_e$	0.9012
	$\Delta E_q \sim \Delta E_{xc}$	0.9751	$\Delta E \sim \Delta T_s + \Delta E_e$	0.9938
H_2O_2	$\Delta E_s \sim \Delta E_{xc}$	0.9270	$\Delta T_s \sim \Delta E_e$	0.9729
	$\Delta E \sim \Delta E_s$	0.9915	$\Delta E \sim \Delta T_s$	0.9932
	$\Delta E \sim \Delta E_q$	0.9870	$\Delta E \sim \Delta E_e$	0.9480
	$\Delta E \sim \Delta E_{xc}$	0.9892	$\Delta E \sim \Delta T_s + \Delta E_e$	0.9684
	$\Delta E \sim \Delta NBO_{Steric}$	0.9665	$\Delta E \sim \Delta E_s + \Delta E_q$	0.9815
	$\Delta E \sim \Delta E_s + \Delta E_e$	0.9917	$\Delta E \sim \Delta T_s + \Delta E_{xc}$	0.9814
	$\Delta E \sim \Delta E_q + \Delta E_e$	0.9861	$\Delta E \sim \Delta E_{xc} + \Delta E_e$	0.9809
	$\Delta E \sim \Delta E_{xc} + \Delta E_e$	0.9569	$\Delta T_s \sim \Delta E_e$	0.9718
	$\Delta E_q \sim \Delta E_s$	0.9960		
	$\Delta E_q \sim \Delta E_{xc}$	0.9995		
	$\Delta E_s \sim \Delta E_{xc}$	0.9942		
	$\Delta E_{xc} \sim \Delta NBO_{Steric}$	0.9849		

between ΔE and $\Delta T_s + \Delta E_e$ is seen. These results together with other linear relationships specific to each of the systems indicate that (i) the internal rotation barrier height can be attributed to one or a few energy components in all the cases and (ii) in different systems the nature of the effect that governs the nature of the barrier height is different. Also, we observe strong correlations from both of the energy partition schemes, Eqs. (14) and (15), suggesting that both can be employed for understanding the nature of the internal rotation barrier. To be more specific, we found five occasions where the total energy difference ΔE strongly correlates with the fermionic quantum energy difference ΔE_q , four times $\Delta E \sim \Delta T_s$, three times $\Delta E \sim \Delta E_e$ and $\Delta E \sim \Delta E_{xc}$, and two times $\Delta E \sim \Delta E_s$ and $\Delta E \sim \Delta NBO_{Steric}$.

V. CONCLUDING REMARKS

The new density-based energy partition scheme proposal in the recent literature,²⁷ for which the total electronic energy

is decomposed into three independent components from three different physiochemical effects, steric, electrostatic, and fermionic quantum, together with the conventional total energy partition scheme, has been applied to six carbon, nitrogen, and oxygen containing molecules with only one rotatable dihedral angle (ethane, methylamine, methanol, hydrazine, hydroxylamine, and hydrogen peroxide) to investigate the nature and origin of the internal rotation barrier height. Two scenarios of the energy difference, relaxed geometry (adiabatic) and fixed geometry (vertical), have been examined. We also compared an alternative definition of the steric energy from NBO analysis. It has been revealed that using the new energy partition scheme, the steric repulsion is usually the smallest for the most stable conformation and larger for less stable conformations, consistent with traditional chemical intuition and in contrast to the results from the other quantification. A number of strongly correlated, linear relationships between the total energy difference and energy component differences for different systems have been unveiled but no universal relationship applicable to all systems studied for both cases has been discovered, indicating that even for simple systems with only one rotatable internal dihedral angle, there exists no omnipresent, unique interpretation on the nature and origin of the internal rotation barrier. We do find, however, that for the vertical case there is a unique linear relationship applicable to all the six molecules between the total energy difference and the sum of the kinetic and electrostatic energy differences. For the adiabatic case, the total potential energy difference is found to correlate well with the total energy difference except for ethane whose rotation barrier is found to be dominated by the quantum effect. Many other strong linear relationships among different energy components have been discovered and can be employed to explain the origin of the barrier height.

ACKNOWLEDGMENTS

The authors are grateful to Robert G. Parr of the University of North Carolina and Paul W. Ayers of McMaster University, Canada, for their valuable comments and suggestions. The work at Pacific Northwest National Laboratory (PNNL) was supported by the U.S. Department of Energy under Contract No. DE-AC06-76RLO 1830 (Office of Biological and Environmental Research, Environmental Molecular Sciences Laboratory operations). The Pacific Northwest National Laboratory is operated by the Battelle Memorial Institute. The Environmental Molecular Sciences Laboratory operations are supported by the DOE's Office of Biological and Environmental Research. This work was partly supported by the National Institutes of Health (Grant No. HL-06350) and NSF (Grant No. ITP/APS-0121361). We acknowledge the use of the computational resources provided by ITS/RENCI at UNC-CH and the Biomedical Unit of the PSC.

¹R. E. Wyatt and R. G. Parr, *J. Chem. Phys.* **43**, S217 (1965).

²R. E. Wyatt and R. G. Parr, *J. Chem. Phys.* **44**, 1529 (1966).

³M. M. Zaalberg, *Theor. Chim. Acta* **5**, 79 (1966).

⁴A. Fadiel, K. D. Eichenbaum, A. Hamza, O. Tan, H. H. Lee, and F. Naftolin, *Current Protein & Peptide Science* **8**, 29 (2007).

⁵T. A. Kufer, *Molecular Biosystems* **4**, 380 (2008).

- ⁶ A. J. Levine, W. W. Hu, Z. H. Feng, and G. Gil, *Ann. N.Y. Acad. Sci.* **1115**, 32 (2007).
- ⁷ Y. R. Mo and J. L. Gao, *Acc. Chem. Res.* **40**, 113 (2007).
- ⁸ F. M. Bickelhaupt and E. J. Baerends, *Angew. Chem., Int. Ed.* **42**, 4183 (2003).
- ⁹ E. J. Baerends, *Nachrichten Aus Der Chemie* **52**, 581 (2004).
- ¹⁰ J. Grunenberg, *Nachrichten Aus Der Chemie* **52**, 831 (2004).
- ¹¹ Y. R. Mo, W. Wu, L. C. Song, M. H. Lin, Q. Zhang, and J. L. Gao, *Angew. Chem., Int. Ed.* **43**, 1986 (2004).
- ¹² P. Schreiner, *Nachrichten Aus Der Chemie* **52**, 581 (2004).
- ¹³ N. Sadlej-Sosnowska, *J. Phys. Chem. A* **107**, 8671 (2003).
- ¹⁴ L. Goodman, V. Pophristic, and W. Wang, *Int. J. Quantum Chem.* **90**, 657 (2002).
- ¹⁵ P. R. Schreiner, *Angew. Chem., Int. Ed.* **41**, 3579 (2002).
- ¹⁶ V. Pophristic and L. Goodman, *Nature (London)* **411**, 565 (2001).
- ¹⁷ R. S. Mulliken, *Tetrahedron* **5**, 253 (1959).
- ¹⁸ R. G. Parr, P. W. Ayers, and R. F. Nalewajski, *J. Phys. Chem. A* **109**, 3957 (2005).
- ¹⁹ V. F. Weisskopf, *Science* **187**, 605 (1975).
- ²⁰ A. E. Reed and F. Weinhold, *Isr. J. Chem.* **31**, 277 (1991).
- ²¹ F. Weinhold, *Angew. Chem., Int. Ed.* **42**, 4188 (2003).
- ²² W. L. Luken and D. N. Beratan, *Theor. Chim. Acta* **61**, 265 (1982).
- ²³ W. L. Luken and J. C. Culberson, *Theor. Chim. Acta* **66**, 279 (1984).
- ²⁴ W. L. Luken, *Croat. Chem. Acta* **57**, 1283 (1984).
- ²⁵ E. V. Ludena, J. M. Ugalde, X. Lopez, J. Fernandez-Rico, and G. Ramirez, *J. Chem. Phys.* **120**, 540 (2004).
- ²⁶ D. L. Cooper and R. Ponc, *Phys. Chem. Chem. Phys.* **10**, 1319 (2008).
- ²⁷ S. B. Liu, *J. Chem. Phys.* **126**, 244103 (2007).
- ²⁸ R. G. Parr and W. Yang, *Density-Functional Theory of Atoms and Molecules* (Clarendon, Oxford, England, 1989).
- ²⁹ R. F. W. Bader, *Atoms in Molecules: A Quantum Theory* (Clarendon, Oxford, 1990).
- ³⁰ S. B. Liu and N. Govind, *J. Phys. Chem. A* **112**, 6690 (2008).
- ³¹ L. Pedersen and K. Morokuma, *J. Chem. Phys.* **46**, 3941 (1967).
- ³² L. C. Song, M. H. Liu, W. Wu, Q. Zhang, and Y. R. Mo, *J. Chem. Theory Comput.* **1**, 394 (2005).
- ³³ I. A. Shlygina, V. Z. Gabdrakipov, and O. V. Agashkin, *Zh. Fiz. Khim.* **57**, 450 (1983).
- ³⁴ J. D. Kemp and K. S. Pitzer, *J. Chem. Phys.* **4**, 749 (1936).
- ³⁵ C. F. von Weizsäcker, *Z. Phys.* **96**, 431 (1935).
- ³⁶ A. Holas and N. H. March, *Phys. Rev. A* **44**, 5521 (1991).
- ³⁷ A. Nagy and N. H. March, *Phys. Chem. Liq.* **25**, 37 (1992).
- ³⁸ A. Nagy and N. H. March, *Phys. Chem. Liq.* **38**, 759 (2000).
- ³⁹ A. Nagy and C. Amovilli, *J. Chem. Phys.* **128**, 114115 (2008).
- ⁴⁰ J. Taruna, J. Piekarewicz, and M. A. Perez-Garcia, *J. Phys. A* **41**, 035308 (2008).
- ⁴¹ S. B. Liu, V. Karasiev, R. Lopez-Boada, and F. De Proft, *Int. J. Quantum Chem.* **69**, 513 (1998).
- ⁴² S. B. Liu and R. G. Parr, *J. Phys. Chem. A* **111**, 10422 (2007).
- ⁴³ S. B. Liu, R. C. Morrison, and R. G. Parr, *J. Chem. Phys.* **125**, 174109 (2006).
- ⁴⁴ S. B. Liu and R. G. Parr, *Phys. Rev. A* **53**, 2211 (1996).
- ⁴⁵ R. G. Parr, S. B. Liu, A. A. Kugler, and A. Nagy, *Phys. Rev. A* **52**, 969 (1995).
- ⁴⁶ S. B. Liu and R. G. Parr, *Phys. Rev. A* **55**, 1792 (1997).
- ⁴⁷ A. Nagy and S. B. Liu, *Phys. Lett. A* **372**, 1654 (2008).
- ⁴⁸ A. Nagy, *Chem. Phys. Lett.* **449**, 212 (2007).
- ⁴⁹ S. B. Liu, P. W. Ayers, and R. G. Parr, *J. Chem. Phys.* **111**, 6197 (1999).
- ⁵⁰ S. B. Liu, *J. Chem. Phys.* **126**, 191107 (2007).
- ⁵¹ R. J. Boyd, *Nature (London)* **310**, 480 (1984).
- ⁵² K. V. Darvesh and R. J. Boyd, *J. Chem. Phys.* **87**, 5329 (1987).
- ⁵³ K. V. Darvesh and R. J. Boyd, *J. Chem. Phys.* **90**, 5638 (1989).
- ⁵⁴ K. V. Darvesh, P. D. Fricker, and R. J. Boyd, *J. Phys. Chem.* **94**, 3480 (1990).
- ⁵⁵ S. B. Liu and W. Langenaeker, *Theor. Chem. Acc.* **110**, 338 (2003).
- ⁵⁶ A. G. Zhong and S. B. Liu, *J. Theor. Comput. Chem.* **4**, 833 (2005).
- ⁵⁷ S. B. Liu and Y. X. Yu, *J. Mol. Struct.: THEOCHEM* **81**, 115 (1991).
- ⁵⁸ S. B. Liu, X. Y. Liu, Q. S. Yang, and Y. X. Yu, *J. Mol. Struct.: THEOCHEM* **83**, 271 (1991).
- ⁵⁹ C. Y. Rong, S. X. Lian, D. L. Yin, B. Shen, A. G. Zhong, L. Bartolotti, and S. B. Liu, *J. Chem. Phys.* **125**, 174102 (2006).
- ⁶⁰ D. E. Bernholdt, E. Apra, H. A. Fruchtl, M. F. Guest, R. J. Harrison, R. A. Kendall, R. A. Kutteh, X. Long, J. B. Nicholas, J. A. Nichols, H. L. Taylor, and A. T. Wong, *Int. J. Quantum Chem.* **56**, 475 (1995).
- ⁶¹ A. D. Becke, *J. Chem. Phys.* **98**, 1372 (1993).
- ⁶² C. T. Lee, W. T. Yang, and R. G. Parr, *Phys. Rev. B* **37**, 785 (1988).
- ⁶³ T. H. Dunning, *J. Chem. Phys.* **90**, 1007 (1989).
- ⁶⁴ A. E. Reed, L. A. Curtiss, and F. Weinhold, *Chem. Rev. (Washington, D.C.)* **88**, 899 (1988).
- ⁶⁵ T. Kasuya and T. Kojima, *J. Phys. Soc. Jpn.* **18**, 364 (1963).
- ⁶⁶ J. M. Flaud, C. Camypeyret, J. W. C. Johns, and B. Carli, *J. Chem. Phys.* **91**, 1504 (1989).
- ⁶⁷ J. K. Badenhoop and F. Weinhold, *Int. J. Quantum Chem.* **72**, 269 (1999).